

Tailoring the tribological properties of nanostructured carbon films under water lubrication

Lei YANG^{1,*}, Shaoshan XIN², Jiang GENG¹, Meiling GUO³

¹ Key Laboratory of Education Ministry for Modern Design & Rotor-Bearing System, Xi'an Jiaotong University, Xi'an 710049, China

² Xi'an Aerospace Propulsion Institute, Xi'an 710100, China

³ School of Mechanical and Precision Instrument Engineering, Xi'an University of Technology, Xi'an 710048, China

Received: 12 October 2022 / Revised: 23 November 2022 / Accepted: 20 December 2022

© The author(s) 2022.

Abstract: Carbon films have been considered suitable to be applied in water lubrication since they exhibit excellent friction-reducing and wear resistance, chemical inertness, etc. However, the basic understanding of tribological behaviors of carbon-based films under water lubrication still needs to be explored. In the present work, carbon films with different nanostructures were prepared by the electron cyclotron resonance (ECR) plasma nano-surface manufacturing system, and micro-textures with different sizes were prepared on the surface of carbon films by plasma etching. The influence of nanostructure and surface texture on the tribological properties of carbon films was investigated. The results show that different nanostructured carbon films can obtain lower friction coefficients and longer wear life under water lubrication than under dry condition. Due to low surface roughness, high hardness, and compact structure, the tribological properties of amorphous carbon (a-C) films under water lubrication are much better than those of graphene sheet-embedded carbon (GSEC) films. The prepared surface texture has a negative effect on the hard a-C film, but it can make the soft GSEC film generate soft wear debris at the initial stage. With the action of water, the soft wear debris is bonded on the surface of the contacting ball to form a silt-like transfer film, which increases the wear life by nearly three orders of magnitude. These results extend the basic understanding of the tribological behavior of carbon film under water lubrication, which is crucial in both fundamental and applied science.

Keywords: water lubrication; carbon film; nanostructure; surface texture; tribological properties

1 Introduction

Compared with the traditional oil lubrication system, the water lubrication system is environment-friendly and has high energy efficiency. However, the low viscosity of water and the friction chemical reaction between metal friction pairs and water limit its wide application. Researchers turned their attention to depositing films that have good water lubrication performance on metal or other substrates, combining the advantages of substrates and films to improve the tribological performance of friction pairs in

water environment. Due to the excellent friction-reducing and wear resistance, chemical inertness, and biocompatibility [1–3], carbon-based films stand out among many films and are widely used in basic machinery, biomedicine, and other fields [4–6]. However, the interaction mechanism between water and carbon film is complex in the friction process, e.g., water molecules would infiltrate into the film [7, 8], resulting in internal extrusion failure of carbon film and falling off from the interface between film and substrate. In addition, water may wash away the wear debris in the contact area and inhibit the formation of transfer

* Corresponding author: Lei YANG, E-mail: yanglxjtu@xjtu.edu.cn

film [9]. Therefore, the basic understanding of the tribological behaviors of carbon-based films under water lubrication still needs to be explored.

Plenty of efforts have been made to enhance the performance of carbon films under water lubrication. Regulating nanostructures of carbon film is one of the most important strategies. Wang et al. [10, 11] found that by adjusting the preparation parameters, such as bias voltage and target power, the graphite-like carbon films with hard and dense structure can be obtained, which can effectively improve the tribological properties of carbon films under water lubrication. Besides, texturing [12–14], element doping [15–17], and intermediate layer [18–20] are also adopted to further improve the tribological properties of carbon films under water lubrication, among which texturing is widely studied because it does not change the chemical compositions of carbon films. It is found that the shape, size, and depth of texture exert important influences on the tribological properties of carbon films under water lubrication [21–23]. It is usually believed that texture can store wear debris as well as store water to produce hydrodynamic lubrication. However, the underlying relationship between the nanostructure of carbon film and the tribological properties under water lubrication is still not clarified. And the effect of water and texture on the accumulation of wear debris and the formation of transfer film is rarely considered.

In this study, different nanostructured carbon films were prepared by the electron cyclotron resonance (ECR) plasma nano-surface fabrication system, and surface textures were fabricated on the film by the ECR plasma etching technology. The tribological properties of carbon films with different nanostructures under water lubrication were studied to explore the influence mechanism of the film nanostructure on the tribological properties under water environment. The generation mechanism of wear debris and transfer film with the combined action of surface texture and water was further investigated to clarify the influence mechanism of surface texture on the tribological properties of carbon film. The research results are of great significance to the coating design and application of friction pair surfaces in the water environment.

2 Experimental

2.1 Preparation of carbon films

In this study, the preparation of carbon films and surface textures was realized by an ECR plasma nano-surface fabrication system. The principle of the ECR-assisted irradiation deposition technology is shown in Fig. 1(a). The first step is to prepare carbon films with different nanostructures. The preparation process and principle are briefly introduced as follows: P-type Si with a thickness of $525 \pm 20 \mu\text{m}$ and resistivity of $7\text{--}13 \Omega\cdot\text{cm}$ was selected as the substrate ($20 \text{ mm} \times 20 \text{ mm}$). The silicon wafer was ultrasonically cleaned with the mixed solution of acetone and ethanol, and then placed in the chamber of the ECR system. Before preparation, the pressure of the chamber was pumped to $5.00 \times 10^{-4} \text{ Pa}$, and then the pressure was raised to $4.00 \times 10^{-2} \text{ Pa}$ by injecting argon gas. Combining with microwave (2.45 GHz , 200 W) and magnetic field composed of double coils (the current is 420 A , and the distance of coils is 390 mm), electrons gain energy and are accelerated, and eventually realized the cyclotron resonance between magnetic mirrors to excite more gas molecules to be ionized to produce

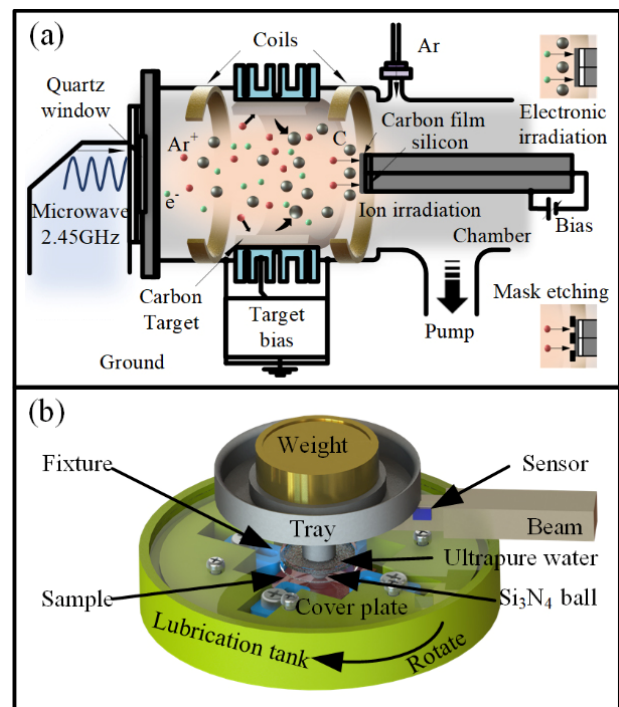


Fig. 1 (a) Principle of ECR plasma nano-surface manufacturing system and (b) schematic of friction test under water lubrication.

plasma. The carbon target was bombarded by Ar^+ with a -300 V bias to excite carbon atoms. Then, carbon atoms are deposited on the substrate surface by adjusting the substrate bias to attract particles with different properties and energies (Ar^+/e^-) to obtain carbon films with different nanostructures. According to Refs. [24, 25], graphene sheet-embedded carbon (GSEC) films were obtained when the substrate bias exceeds 40 V. Amorphous carbon films were obtained when the substrate bias is lower than 40 V. The reasons for the structural changes and the division basis are shown in the characterizations of carbon films below. Preparation parameters for depositing carbon films are shown in Table 1.

The second step is to prepare surface texture on the prepared carbon film by the ECR plasma etching technology. The target bias is not applied during the etching process. A bias of -100 V is applied to the substrate to attract Ar^+ to bombard the surface of the carbon film for etching. In order to selectively etch the specific area of carbon film, a mask with holes fabricated by photolithography electroforming is placed on its surface. Ar^+ passes through the holes and bombards the exposed surface of carbon film, and thus ion etching is performed on the specified area, while the covered part remains the same [26, 27]. By controlling the hole diameter of the mask, the surface texture of regular circular pits with different diameters can be obtained. For the depth, the etching rate of the carbon film is 1 nm/min. Therefore, the depth of the texture can be determined according to the etching time. The parameters of the etching are shown in Table 1.

Table 1 Preparation parameters of carbon films.

	Amorphous carbon (a-C) film			GSEC film	
Substrate bias (V)	-10	5	20	50	100
Film thickness (nm)	100	100	100	100	100
Texture diameter (μm)	10, 60, and 120				
Texture depth (nm)	10, 30, and 60				

2.2 Carbon film characterization and friction test

The Raman spectra (HR-Resolution, HORIBA) with 532 nm laser were used to obtain the information

of D peak and G peak in the spectral region of 1,000–3,500 nm, and then the size of the nanocrystalline graphene sheet was calculated. The nanostructures of carbon film were observed by the transmission electron microscopy (TEM; JEM-2100, JEOL) at a 200 kV electron acceleration voltage. The reflection spectra of the carbon atoms were measured by the X-ray photoelectron spectroscopy (XPS; AXIS ULtrabltd), and the hybridization modes of carbon atoms were analyzed. The surface texture was characterized by the tungsten filament scanning electron microscopy (SEM; EVO 10, Carl Zeiss).

The tribological properties of carbon film in water environment were tested using a ball-on-disk tribometer (BS-TR071, SCILAND Co.). A Si_3N_4 ball with a radius of 3.17 mm was sliding against the carbon film. The rotation speed was 180 r/min (friction radius: 1.4 mm), and the normal load was 1 N. Three repeated tests were performed on each sample to obtain the average results. In order to measure the tribological properties in water environment, a sealed lubricating tank was designed and installed on the tribometer, as shown in Fig. 1(b). During the whole test process, the carbon film and the ball were completely immersed in the water.

In order to analyze the tribological behavior of carbon films with different nanostructures in water environment, the structures and mechanical properties of carbon films were characterized. The surface roughness of the carbon films were measured by the atomic force microscopy (AFM; INNOVA, BRUKER). The hardness of the films were measured by a nanoindenter (TI 950, Bruker). The Berkovich indenter with a curvature radius of 100 nm was used in the test, and the maximum indentation load was 900 μN . The densities of two typical amorphous and GSEC films were measured by the X-ray reflectometry (XRR; Empyrean). In order to further study the effect of surface texture on the tribological properties of carbon films in water environment, the morphologies of wear debris and transfer films formed on Si_3N_4 ball after the friction tests were observed by the optical microscope (Axioscope 5, Carl Zeiss). Then water samples containing wear debris in the tank after the friction tests were collected, and the size of the debris was measured by a nanoparticle size analyzer (Zetasizer Nano ZSE, Malvern).

3 Results and discussion

3.1 Nanostructures of carbon films

The TEM images of typical nanostructured carbon films prepared under different substrate bias voltages are shown in Fig. 2. It can be found that the carbon atoms in the film prepared at the substrate bias of 20 V are arranged in disorder. Figure 3(a) shows that the D peak and G peak in the Raman spectrum of the 20 V carbon film cannot be clearly distinguished. By fitting the curve and integrating the peak area, it is found that the I_D/I_G (the intensity ratio of D peak to G peak) is only 0.56. The sp^2/sp^3 ratio is only 0.77 according to the XPS results, as shown in Fig. 3(b), which further confirms that the carbon atoms are mainly sp^3 hybridized and randomly arranged. Based on the above analysis, the 20 V carbon film is a typical amorphous carbon film. When the substrate bias increases to 50 V, a few layered stacked graphene sheets appear in the TEM image, as shown in the red

circle in Fig. 2. The I_D/I_G ratio and sp^2/sp^3 ratio also increase. When the substrate bias finally increases to 100 V, more layered stacked nanocrystalline graphene sheets appear in the TEM images, which are uniformly distributed. Accordingly, its Raman curve shows the most obvious D peak and G peak with the I_D/I_G ratio increasing to 1.16. And the sp^2/sp^3 ratio increases to 5.72. These all support the formation of a large number of nanocrystalline graphene sheets. Therefore, this kind of carbon film is named as the GSEC film. Besides, the size of the graphene sheets can be calculated by Eq. (1) [28, 29]:

$$I_D / I_G = C(\lambda)L_\alpha^2 \quad (1)$$

where $C(\lambda)$ is a constant related to the laser wavelength, which is 0.55 nm^{-2} when the laser wavelength is 532 nm, and L_α is the length of the graphene sheets. Since the I_D/I_G increases with the increase of the substrate bias, the calculated size of nanocrystalline also increases. This is consistent with the above analysis.

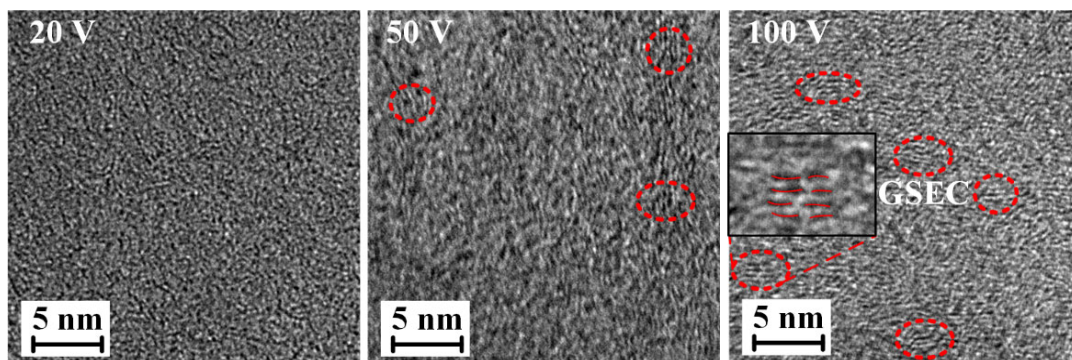


Fig. 2 TEM images of carbon films prepared under different substrate bias voltages.

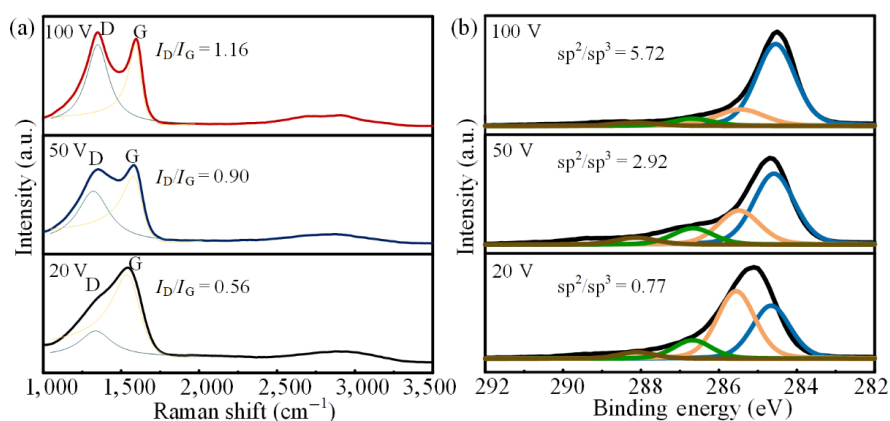


Fig. 3 (a) Raman spectra and (b) XPS spectra of carbon films prepared under different substrate bias voltages.

3.2 Tribological properties of carbon films in water

Figure 4 shows the tribological properties of carbon films prepared with different substrate bias voltages under dry and water lubrication conditions. Figures 4(a) and 4(b) are the friction curves of a-C film prepared with the bias voltage of 20 V and GSEC film prepared with the bias voltage of 100 V, respectively. It can be seen from Fig. 4(a) that the friction coefficient of 20 V a-C film suddenly increases from 0.098 to 0.750 after 4,460 wear cycles, corresponding to the observation of the damage and spalling of the carbon film under the optical microscope. Therefore, it is considered that the frictional cycle at this time is the wear life of the carbon film. Moreover, the wear life of 20 V carbon film is extremely long in water environment. The friction coefficient remains stable at 0.077 within 15,000 cycles. Thus, the wear life is considered to be longer than 15,000 cycles (the same as below). In comparison, even under water lubrication, the wear life of 100 V GSEC film is only 18 cycles, and the friction coefficient is 0.120. The test results of carbon films with different bias voltages in dry friction and water environment are summarized in Figs. 4(c) and 4(d). It is obvious that the presence of water reduces

the friction coefficient of all carbon films and prolongs their wear life. Furthermore, the tribological properties of a-C films (−10, 5, and 20 V) are all better than those of GSEC films (50 and 100 V).

The underlying mechanism for the effect of nanostructure on tribological properties of carbon films in water is further explored. Figure 5(a) presents the surface roughness of carbon films prepared with typical substrate bias voltages. The roughness of the film increases with the increase of the bias voltage. The roughness of GSEC films prepared with a bias voltage of 100 V reaches the maximum value (14.1 nm). Figure 5(b) is the hardness of carbon films with different bias voltages. The hardness of Si substrate (11.34 GPa) is between a-C film and GSEC film. 5 V carbon film and 100 V carbon film have the maximum (18.37 GPa) and minimum (7.67 GPa) hardness, respectively. The wear scars of 20 and 100 V carbon films after being rubbed by the ball were observed by an optical microscope (Axio Scope.A1, ZEISS), as shown in Fig. 6. It can be found that the wear scar of 20 V carbon film presents several grooves produced by the extrusion of hard wear debris by ball. The wear scar of 100 V carbon film presents the accumulation and aggregation of soft wear debris.

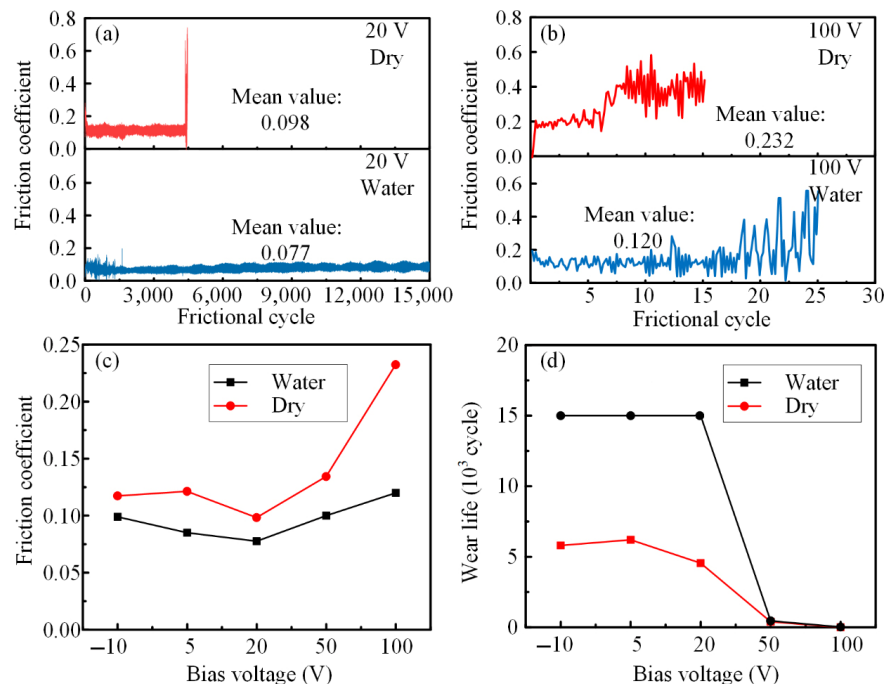


Fig. 4 Tribological properties of different nanostructured carbon films under dry friction and water lubrication. (a) Friction curves of 20 V carbon films, (b) friction curves of 100 V carbon films, (c) friction coefficients of carbon films prepared by different bias voltages, and (d) wear life of carbon films prepared by different bias voltages.

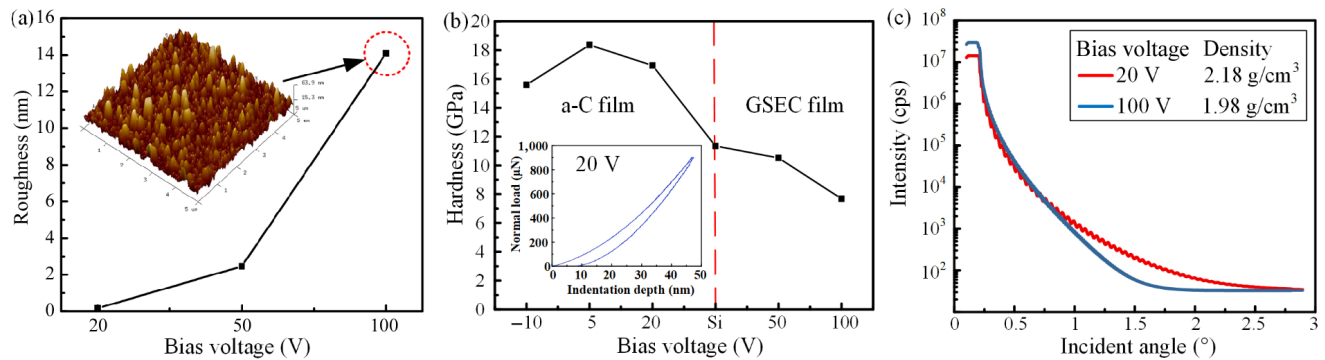


Fig. 5 (a) Surface roughness and (b) hardness of carbon films prepared by different bias voltages and (c) XRR reflection intensity curves of 20 and 100 V carbon films.

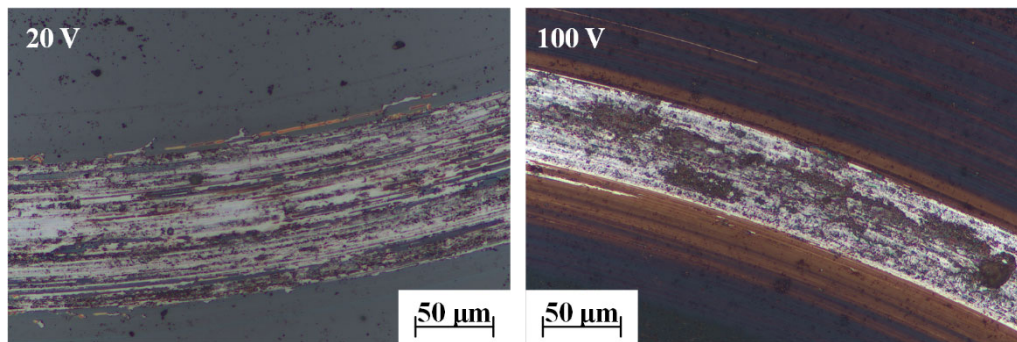


Fig. 6 Optical images of wear scars on 20 and 100 V carbon films

Since the density of the film could affect the interaction between water and the film during the tribological process, we measured the densities of two typical amorphous and GSEC films by the XRR, as shown in Fig. 5(c). When the incident angle is the same, the stronger the reflection intensity is, the larger the density of the film is. It can be seen from Fig. 5(c) that the reflection intensity curve of a-C film prepared with a bias voltage of 20 V is above that of GSEC film prepared with a bias voltage of 100 V, i.e., the reflection intensity is larger. Further calculation based on the curves shows that the density of 20 V a-C film (2.18 g/cm^3) is more than 10% larger than that of 100 V GSEC film (1.98 g/cm^3).

The above analysis shows that the a-C film has lower surface roughness and higher hardness and compactness than the GSEC film. In Refs. [30, 31], graphene sheets are formed due to the inelastic scattering of low energy electrons. The existence of graphene sheets in carbon film results in more sp^2 bonds, and hence the hardness of GSEC film is lower. Meanwhile, regions containing graphene sheets in the film exhibit higher electrical conductivity than

other amorphous regions. As a result, during the film growth process, the ability to attract electrons and carbon atoms is locally enhanced, resulting in rapid deposition in these regions containing graphene sheets. Therefore, the GSEC film presents larger roughness and looser structure. Consequently, the tribological property is poorer than that of a-C film. Moreover, denser a-C film can effectively inhibit the infiltration of water molecules. On the one hand, it can resist the internal extrusion damage of water molecules on the carbon film. On the other hand, it can prevent the carbon film from falling off from the film–substrate interface.

In order to further clarify the role of water during the tribological process, friction tests under dry and water lubrication conditions were performed on 20 V a-C films and stopped at 3,000 cycles. Then the contents of C and O elements in the wear scar were analyzed by the XPS, as shown in Fig. 7. The carbon films were dried at room temperature for a week before the XPS test to eliminate the influence of water molecules remaining on the surface. The mass fraction of O element under water lubrication (22.58%) is two

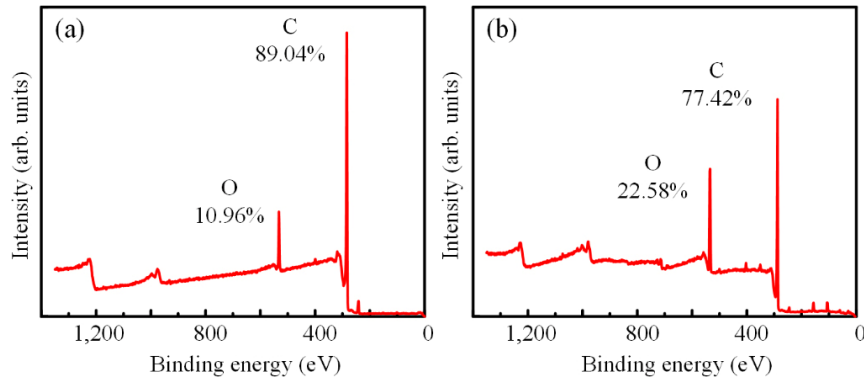


Fig. 7 XPS spectra of wear scars on 20 V a-C film under (a) dry friction and (b) water lubrication.

times larger than that under dry friction (10.96%). This indicates that the friction chemical reaction occurs in the friction process, which may form oxygen-containing groups such as hydroxyl and carboxyl. These groups can improve the hydrophilicity of the carbon film in the contact area, and thus more water lubricating layer can be stored at the contact interface.

Then, the tribological properties of a-C films prepared with substrate bias voltages of -10 , 5 , and 20 V under different normal loads in water were further studied. The test results are shown in Fig. 8. It can be seen that the friction coefficient of a-C film in water environment decreases with the increase of normal load. And the friction coefficient of -10 V a-C film decreases the most obviously, which changes from 0.099 to 0.056 . Moreover, the wear life of 20 V a-C film under 5 N normal load can still reach $11,450$ cycles, which shows the applicative prospect under heavy loads. The dependence of friction on the

normal load can be explained by a shear mechanism accommodating the sliding motion [32, 33]. When the ball-on-disk contact conforms to the Hertzian elastic contact model, the friction coefficient decreases as the normal load increases.

3.3 Effect of surface texture on tribological properties of carbon films in water

Figure 9 shows the SEM images of the textured carbon films. Patterns on the mask can be reproduced completely by the etching process. The radial dimension of the texture can be precisely controlled at the micron level, i.e., 10 , 60 , and 120 μm through-hole apertures of the mask, and the corresponding circular pit textures with diameters of 10 , 60 , and 120 μm are obtained on the carbon film. The depth can be controlled by changing the etching time, and the etching depths are 10 , 30 , and 60 nm. Textures were fabricated on typical a-C (substrate bias: 20 V) and GSEC (substrate bias: 100 V) films. In the subsequent expression, the textured

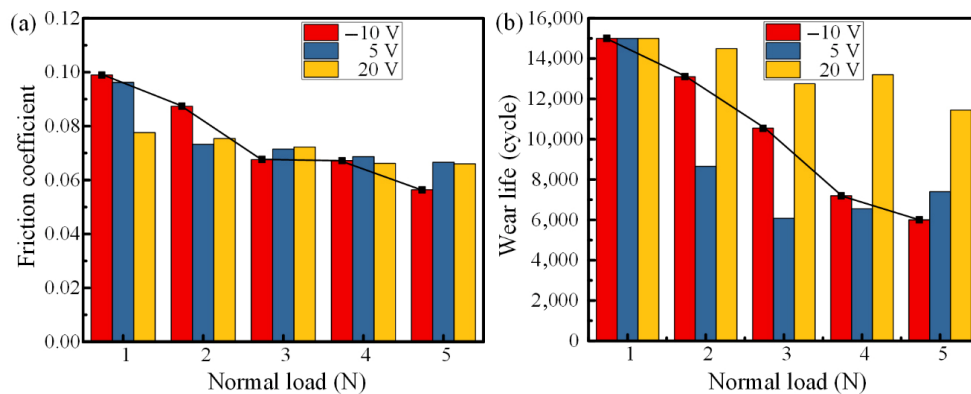


Fig. 8 Tribological properties of a-C films in water under different normal loads. (a) Variation of friction coefficient and (b) variation of wear life.

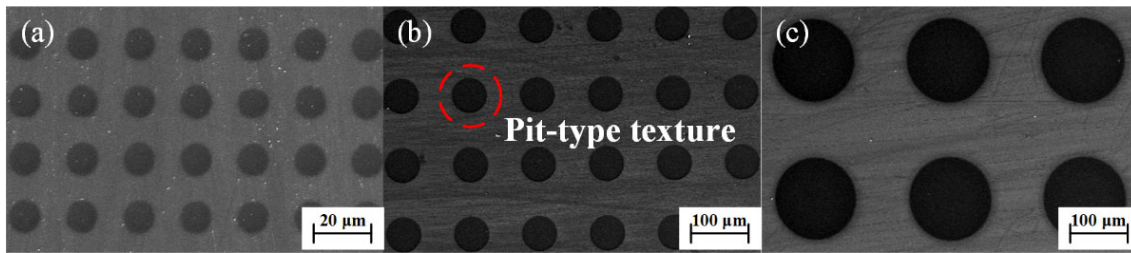


Fig. 9 SEM images of carbon films with (a) texture of 10 μm diameter, (b) texture of 60 μm diameter, and (c) texture of 120 μm diameter.

parameters are named as “diameter of texture–depth of texture”. For example, the texture with a diameter of 120 μm and depth of 30 nm is abbreviated to 120 μm –30 nm.

Figure 10(a) shows the friction curves of the textured 20 V a-C films under water lubrication. It is obvious that the wear life of 20 V a-C film is shortened when 120 μm –30 nm surface texture is fabricated. The wear life decreases from more than 15,000 to 5,850 cycles, and the average friction coefficient increases from 0.077 to 0.111 with a larger fluctuation. For films with other texture parameters, the results are illustrated in Figs. 10(b) and 10(c) (where ★ represents the test results of the film without texture). We can see that the friction coefficients of the textured films are all larger than that of the

original film. Moreover, the wear life of the film decreases when the texture is fabricated. Moreover, with the increase of the texture diameter, the friction coefficient of 20 V a-C film increases, and its wear life decreases under water lubrication. In order to explain the mechanism of tribological performance degradation induced by the surface texture, a schematic is presented, as shown in Fig. 10(d). During the friction process, stress concentration occurs at the top and bottom corners of the texture, generating hard wear debris. The debris cannot be completely washed away by water and will still remain partially at the contact interface. The hard wear debris plays a negative role in the friction process, resulting in a general degradation in the tribological properties of the a-C films.

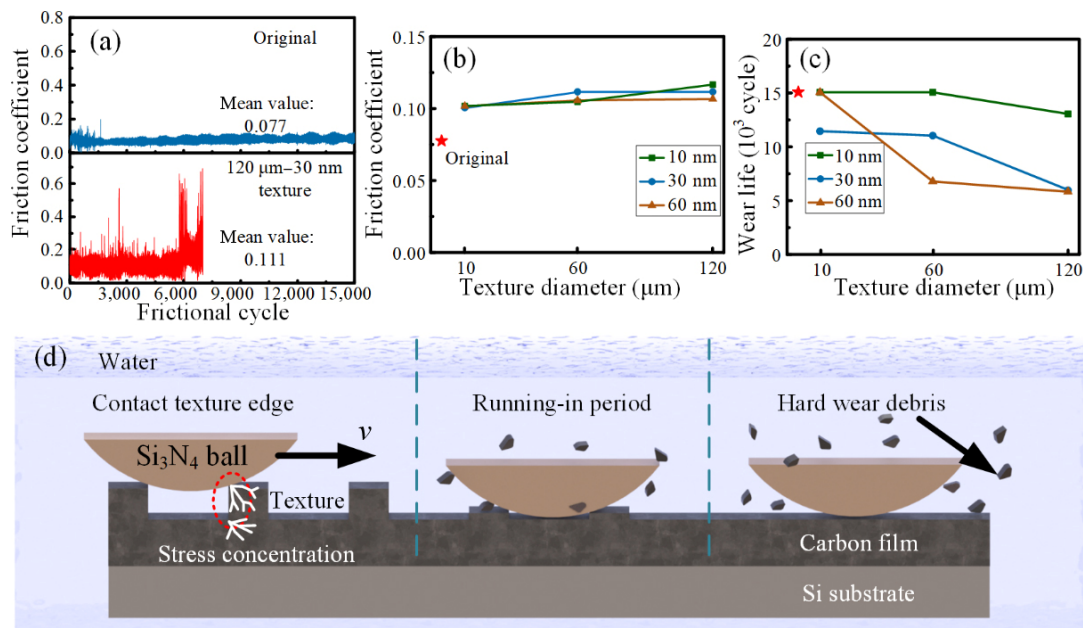


Fig. 10 (a) Friction curves of original 20 V carbon film and textured film (120 μm –30 nm), (b) friction coefficients and (c) wear life of 20 V carbon film with different texture diameters, and (d) schematic of influencing mechanism of surface texture on tribological properties of 20 V carbon film under water lubrication. Note: v in (d) represents the speed.

In order to verify the above mechanism, the contact area of Si_3N_4 ball sliding against $120\ \mu\text{m}$ – $30\ \text{nm}$ textured $20\ \text{V}$ a-C film was observed by the optical microscope after 300 cycles of friction test under dry and water lubrication conditions. As shown in Figs. 11(a) and 11(b), a part of the wear debris was attached to the surface of the ball under dry friction. Under the grinding effect of the ball and carbon film, some hard wear debris was crushed and bonded to the surface of the ball to form a thin transfer film. In comparison, under water lubrication, the amount of wear debris attached to the ball surface is significantly reduced, and there is no transfer film formed, resulting

in the degradation of the tribological properties of the textured carbon film under water lubrication. This confirms the above mechanism that water will wash away part of the hard wear debris. The left hard debris at the contact interface is not easy to be deformed and attached to the surface of the Si_3N_4 ball to form the transfer film.

Figure 12(a) shows the friction curves of the textured $100\ \text{V}$ GSEC films under water lubrication. We can find that the wear life of the film is increased by three orders of magnitude after the preparation of $120\ \mu\text{m}$ – $30\ \text{nm}$ surface texture. The friction coefficient is significantly reduced and becomes more stable. For

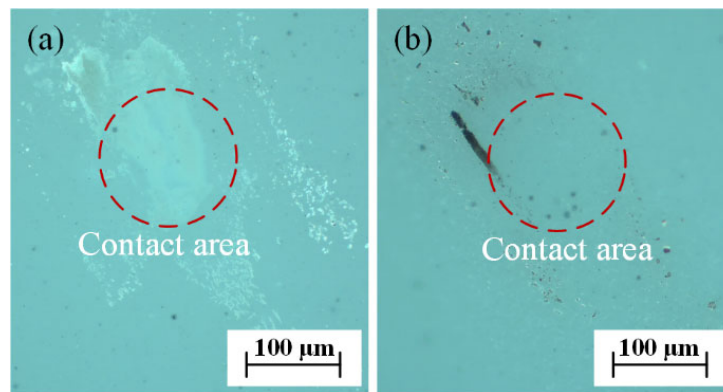


Fig. 11 Optical images of surfaces of Si_3N_4 ball sliding against $120\ \mu\text{m}$ – $30\ \text{nm}$ textured $20\ \text{V}$ a-C film after 300 cycles of friction test under (a) dry and (b) water lubrication conditions.

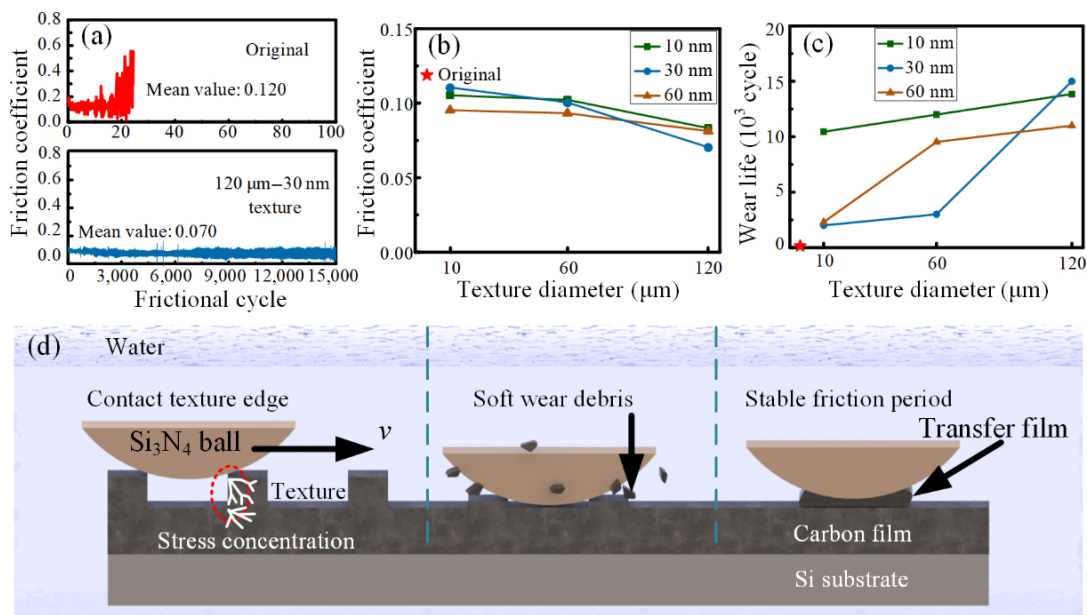


Fig. 12 (a) Friction curves of original $100\ \text{V}$ carbon film and textured film ($120\ \mu\text{m}$ – $30\ \text{nm}$), (b) friction coefficients and (c) wear life of $100\ \text{V}$ carbon film with different texture diameters, and (d) schematic of influencing mechanism of surface texture on tribological properties of $100\ \text{V}$ carbon film under water lubrication.

different texture parameters, it is found that the friction coefficient of 100 V GSEC film decreases, and its wear life increases with the increase of texture diameter, as shown in Figs. 12(b) and 12(c), respectively. The mechanism of the texture effect on the tribological performance of GSEC film is presented in Fig. 12(d). Stress concentration occurs at the texture when the ball passes through the surface texture of the carbon film at the initial stage, resulting in the damage of the texture and the formation of a large number of soft wear debris. The soft debris is prone to being deformed, and the loose structure makes it easy to adsorb water molecules. Therefore, the debris is easier to bond, generating a thick and uniform transfer film on the surface of the ball, which plays a role in reducing friction. Furthermore, it is considered that texture size is closely related to the formation of transfer film. For texture with larger diameters, larger soft wear debris is generated, which is easier to bond together, forming transfer film on the contact ball. Therefore, GSEC films with larger texture sizes exhibit better tribological performance.

In order to verify the above mechanism, an optical

microscope was used to observe the transfer film formed on the Si_3N_4 ball and the wear debris in water when GSEC films with different texture diameters were worn for 300 cycles, as shown in Figs. 13(a)–13(c) and Figs. 13(e)–13(g), respectively. The reason we stopped the tribo-tests at 300 cycles to observe the transfer film is as follows. According to the friction curves of the films, the friction coefficient becomes stable after 200 cycles, indicating that a stable transfer film is generated after 200 cycles. In addition, the wear life of carbon films with a 10 μm diameter is still short. In order to compare the transfer film at the same stage, we stopped the tests at 300 cycles. From Figs. 13(e)–13(g), we can clearly see that the size of wear debris increases with the increase of texture diameter. Accordingly, as seen from Figs. 13(a)–13(c), when the texture diameter is 10 μm , there is no transfer film formed on the ball surface. In comparison, when the texture diameter increases to 120 μm , thick and uniform silt-like transfer film forms on the surface of the ball, which greatly reduces the friction coefficient and wear. Then, the transfer films of 100 V carbon film with the 120 μm –30 nm texture under dry friction and

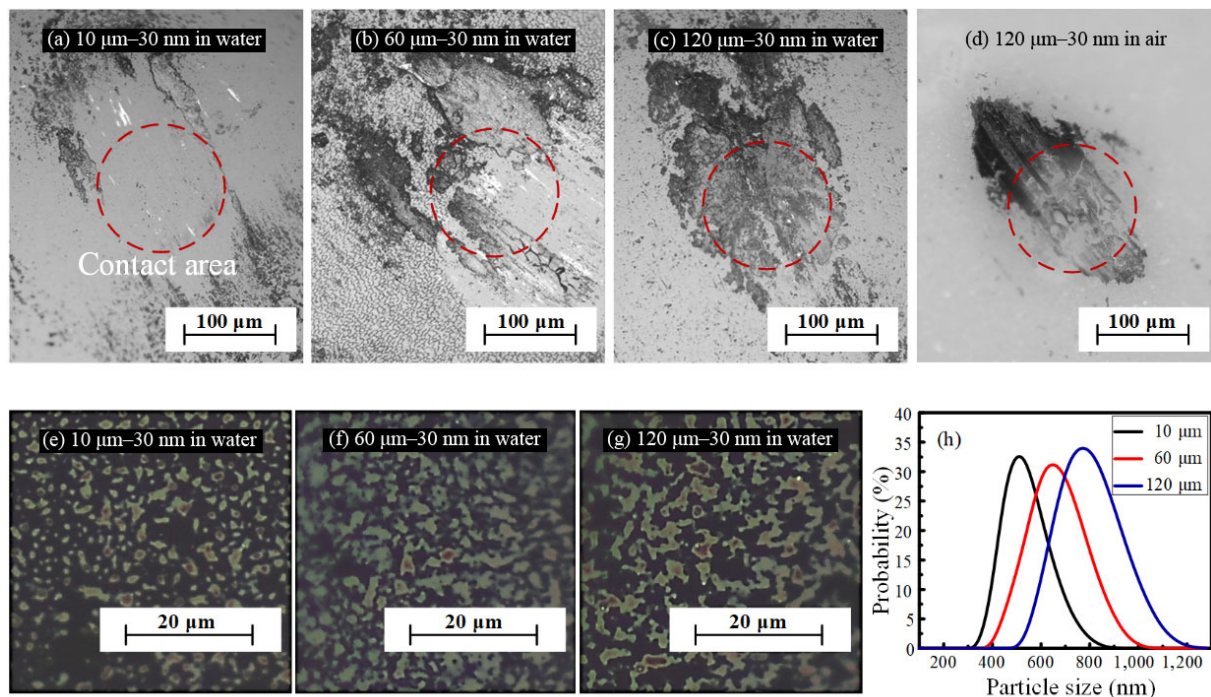


Fig. 13 Optical images of surfaces of Si_3N_4 ball sliding against different textured 100 V carbon films: (a) 10 μm –30 nm in water, (b) 60 μm –30 nm in water, (c) 120 μm –30 nm in water, and (d) 120 μm –30 nm under dry friction. Optical images of wear debris in water for different textured 100 V carbon films: (e) 10 μm –30 nm in water, (f) 60 μm –30 nm in water, and (g) 120 μm –30 nm in water. (h) Particle size distribution curves of wear debris in water for carbon film with different texture diameters.

water lubrication are compared. Transfer film formed under dry friction is far less than that under water lubrication in terms of thickness, uniformity, and coverage area, as shown in Fig. 13(d). Therefore, we believe that water molecules are easy to adsorb on the loose and soft wear debris during the formation of transfer film, which promotes the bonding of soft wear debris. In order to further verify the influence of texture diameter on the size of wear debris, the debris size was quantitatively measured, as shown in Fig. 13(h). The curves are the probability distribution of the debris size. The peak position is closely related to the equivalent size of the debris. It is apparent that the size of the debris increases as the texture diameter increases from 10 to 120 μm , which is consistent with the optical images.

4 Conclusions

To summarize, the tribological properties of carbon films with different nanostructures and surface textures under water lubrication were investigated. It was found that the tribological properties of different nanostructured carbon films were all improved under water lubrication. Due to the low surface roughness, high hardness, and compact structure, a-C film has better tribological properties than GSEC film under water lubrication. Then surface textures with different sizes were fabricated on typical a-C film (bias voltage: 20 V) and GSEC film (bias voltage: 100 V). For 20 V a-C film, a large number of hard wear debris is formed after the surface texture is destroyed in the running-in period. The hard and compact wear debris is not easy to bond in water and adsorbs water molecules to form transfer film, which has a negative effect on the tribological properties of the a-C film. It was further found that the texture was more likely to be destroyed, and the larger size of hard wear debris was generated with the increase of the texture diameter, which result in the degradation of the tribological properties. For the textured 100 V GSEC film, soft wear debris was generated during the running-in period. Water molecules are easy to be adsorbed on soft wear debris and promote it to bond. As a result, a thick and uniform silt-like transfer film was generated on the contacting ball, which plays an effective role in reducing friction and wear. Moreover, larger

texture generated larger wear debris, which is easier to form an effective transfer film. This work extends the basic understanding of the tribological behavior of carbon film under water lubrication and is beneficial to the application of carbon film and texture technique in water environment.

Acknowledgements

The authors thank the National Natural Science Foundation of China (Grant Nos. 52275210 and 51905423), Natural Science Foundation of Shaanxi Province (Grant No. 2022JM-175), the Fundamental Research Funds for the Central Universities, and the scanning electron microscope (SEM) facility of Instrumental Analysis Center of Xi'an Jiaotong University, Xi'an, China.

Declaration of competing interest

The authors have no competing interests to declare that are relevant to the content of this article.

Open Access This article is licensed under a Creative Commons Attribution 4.0 International License, which permits use, sharing, adaptation, distribution and reproduction in any medium or format, as long as you give appropriate credit to the original author(s) and the source, provide a link to the Creative Commons licence, and indicate if changes were made.

The images or other third party material in this article are included in the article's Creative Commons licence, unless indicated otherwise in a credit line to the material. If material is not included in the article's Creative Commons licence and your intended use is not permitted by statutory regulation or exceeds the permitted use, you will need to obtain permission directly from the copyright holder.

To view a copy of this licence, visit <http://creativecommons.org/licenses/by/4.0/>.

References

- [1] Ye Y W, Wang C T, Wang Y X, Liu W, Liu Z Y, Li X G. The influence of different metallic counterparts on the tribological performance of nc-CrC/GLC in seawater. *Surf Coat Tech* **325**: 689–696 (2017)

- [2] Shi X R, Shi Y J, Chen J, Liskiewicz T W, Beake B D, Zhou Z H, Wang Z H, Wu G S. Influence of gradient interlayer thickness on corrosion and tribological behavior of Ti-containing multilayer graphite-like carbon films. *Wear* **488–489**: 204177 (2022)
- [3] Zhang T F, Jiang F, Liao T T, Deng Q Y, Li S S, Wang Y, Leng Y X. Tribological behavior of diamond like carbon film sliding against CoCrMo or Al₂O₃ in air and water environment. *Tribol Int* **95**: 456–461 (2016)
- [4] Wang Y X, Pu J B, Wang J F, Li J L, Chen J M, Xue Q J. Interlayer design for the graphite-like carbon film with high load-bearing capacity under sliding-friction condition in water. *Appl Surf Sci* **311**: 816–824 (2014)
- [5] Litwin W. Influence of local bush wear on water lubricated sliding bearing load carrying capacity. *Tribol Int* **103**: 352–358 (2016)
- [6] Huang J X, Wang L P, Liu B, Wan S H, Xue Q J. *In vitro* evaluation of the tribological response of Mo-doped graphite-like carbon film in different biological media. *ACS Appl Mater Interfaces* **7**(4): 2772–2783 (2015)
- [7] Park S J, Lee K R, Ahn S H, Kim J G. Instability of diamond-like carbon (DLC) films during sliding in aqueous environment. *Diam Relat Mater* **17**(3): 247–251 (2008)
- [8] Chen L, Qian L M. Role of interfacial water in adhesion, friction, and wear—A critical review. *Friction* **9**(1): 1–28 (2021)
- [9] Tokoro M, Aiyama Y, Masuko M, Suzuki A, Ito H, Yamamoto K. Improvement of tribological characteristics under water lubrication of DLC-coatings by surface polishing. *Wear* **267**(12): 2167–2172 (2009)
- [10] Wang Y X, Wang L P, Zhang G G, Wang S C, Wood R J K, Xue Q J. Effect of bias voltage on microstructure and properties of Ti-doped graphite-like carbon films synthesized by magnetron sputtering. *Surf Coat Tech* **205**(3): 793–800 (2010)
- [11] Wang Y X, Li J L, Shan L, Chen J M, Xue Q J. Tribological performances of the graphite-like carbon films deposited with different target powers in ambient air and distilled water. *Tribol Int* **73**: 17–24 (2014)
- [12] Song H, Ji L, Li H X, Liu X H, Zhou H D, Liu L, Chen J M. Superlow friction behavior of surface-textured a-C:H film in water environments. *Tribol T* **58**(5): 867–874 (2015)
- [13] Ding Q, Wang L P, Wang Y X, Wang S C, Hu L T, Xue Q J. Improved tribological behavior of DLC films under water lubrication by surface texturing. *Tribol Lett* **41**(2): 439–449 (2011)
- [14] Ye Y W, Wang C T, Wang Y X, Zhao W J, Li J L, Yao Y R. A novel strategy to enhance the tribological properties of Cr/GLC films in seawater by surface texturing. *Surf Coat Tech* **280**: 338–346 (2015)
- [15] Sutton D C, Limbert G, Stewart D, Wood R J K. The friction of diamond-like carbon coatings in a water environment. *Friction* **1**(3): 210–221 (2013)
- [16] Huang J X, Wan S H, Liu B, Xue Q J. Improved adaptability of PEEK by Nb doped graphite-like carbon composite coatings for bio-tribological applications. *Surf Coat Tech* **247**: 20–29 (2014)
- [17] Sui X D, Xu R N, Liu J, Zhang S T, Wu Y, Yang J, Hao J Y. Tailoring the tribocorrosion and antifouling performance of (Cr,Cu)–GLC coatings for marine application. *ACS Appl Mater Interfaces* **10**(42): 36531–36539 (2018)
- [18] Costa R P C, Lima-Oliveira D A, Marciano F R, Lobo A O, Corat E J, Trava-Airoldi V J. Comparative study of the tribological behavior under hybrid lubrication of diamond-like carbon films with different adhesion interfaces. *Appl Surf Sci* **285**: 645–648 (2013)
- [19] Wang Y X, Pu J B, Wang J F, Li J L, Chen J M, Xue Q J. Interlayer design for the graphite-like carbon film with high load-bearing capacity under sliding-friction condition in water. *Appl Surf Sci* **311**: 816–824 (2014)
- [20] Li L, Guo P, Liu L L, Li X W, Ke P L, Wang A Y. Structural design of Cr/GLC films for high tribological performance in artificial seawater: Cr/GLC ratio and multilayer structure. *J Mater Sci Technol* **34**(8): 1273–1280 (2018)
- [21] Ye Y W, Wang C T, Chen H, Wang Y X, Zhao W J, Mu Y T. Micro/nanotexture design for improving tribological properties of Cr/GLC films in seawater. *Tribol T* **60**(1): 95–105 (2017)
- [22] Ren S M, Huang J X, Cui M J, Pu J B, Wang L P. Improved adaptability of polyaryl-ether-ether-ketone with texture pattern and graphite-like carbon film for bio-tribological applications. *Appl Surf Sci* **400**: 24–37 (2017)
- [23] He D Q, Zheng S X, Pu J B, Zhang G G, Hu L T. Improving tribological properties of titanium alloys by combining laser surface texturing and diamond-like carbon film. *Tribol Int* **82**: 20–27 (2015)
- [24] Wang C, Diao D F, Fan X, Chen C. Graphene sheets embedded carbon film prepared by electron irradiation in electron cyclotron resonance plasma. *Appl Phys Lett* **100**(23): 231909 (2012)
- [25] Chen S C, Qian G C, Yang L. Precise control of surface texture on carbon film by ion etching through filter: Optimization of texture size for improving tribological behavior. *Surf Coat Tech* **362**: 105–112 (2019)
- [26] Diao D F, Wang C, Fan X. Frictional behavior of nanostructured carbon films. *Friction* **1**(1): 63–71 (2013)

- [27] Geng J, Chen S C, Xin S S, Guo Y J, Yang L. Surface/interface texture enhanced tribological properties of graphene sheets embedded carbon films. *Tribol Int* **163**: 107191 (2021)
- [28] Ferrari A C, Robertson J. Interpretation of Raman spectra of disordered and amorphous carbon. *Phys Rev B* **61**(20): 14095–14107 (2000)
- [29] Ferrari A C. Raman spectroscopy of graphene and graphite: Disorder, electron–phonon coupling, doping and nonadiabatic effects. *Solid State Commun* **143**(1–2): 47–57 (2007)
- [30] Chen C, Diao D F, Fan X, Yang L, Wang C. Frictional behavior of carbon film embedded with controlling-sized graphene nanocrystallites. *Tribol Lett* **55**(3): 429–435 (2014)
- [31] Yang L, Qi K, Diao D F, Wang P F, Xue P D. Magnetostrictive friction of graphene sheets embedded carbon film. *Carbon* **159**: 617–624 (2020)
- [32] Mohrbacher H, Celis J P. Friction mechanisms in hydrogenated amorphous carbon coatings. *Diam Relat Mater* **4**(11): 1267–1270 (1995)
- [33] Cui L C, Lu Z B, Wang L P. Environmental effect on the load-dependent friction behavior of a diamond-like carbon film. *Tribol Int* **82**: 195–199 (2015)



Lei YANG. He received his Ph.D. degree in mechanical engineering from Xi'an Jiaotong University, Xi'an, China, in 2014. He is currently an

associate professor at School of Mechanical Engineering, Xi'an Jiaotong University. His research interests include nano-surface engineering and tribology and energy harvesting technology and application.



Shaoshan XIN. He received his master's degree from Xi'an Jiaotong University, Xi'an, China, in 2022, and

now he is an assistant engineer at Xi'an Aerospace Propulsion Institute, Xi'an, China. His research interests are tribology performance on carbon-based materials.



Jiang GENG. He received his bachelor's degree from Liaoning Technical University, Fuxin, China, in 2016, and now he is a Ph.D.

candidate at School of Mechanical and Engineering, Xi'an Jiaotong University Xi'an, China. His research interests are tribology performance on textured carbon-based materials.



Meiling GUO. She received her Ph.D. degree from School of Mechanical Engineering from Xi'an Jiaotong University, Xi'an, China, in 2016. She is currently a lecturer

at School of Mechanical and Precision Instrument Engineering, Xi'an University of Technology, Xi'an, China. Her research interests are nano-surface manufacture and science, nanotribology, and triboelectric nanogenerator.